

# Role of seed layer: lattice orientation attachment and structural stabilization on the lateral growth of ZnO nanorods

R. Devaraj<sup>1</sup> · K. Venkatachalam<sup>1</sup> · P. M. Razad<sup>2</sup>

Received: 7 November 2015 / Accepted: 21 December 2015 / Published online: 29 December 2015  
© Springer Science+Business Media New York 2015

**Abstract** The role of seed layer (SL) on the growth of ZnO nanorods was investigated by preparing SL with different concentrations of zinc acetate by jet nebulizer spray pyrolysis technique at different deposition time. The ZnO nanorods were grown on the ZnO seeded substrate by hydrothermal method. The influence of SL on the growth of ZnO nanorods with respect to SL concentration and deposition time were studied with various characterization tools. The results had shown that the orientation of crystallites and alignment of rods were found to be improved with lower concentration and increasing deposition time of SL and the converse effect was found in the higher concentration. The various morphologies were obtained on the surface of SL with respect to different concentration and deposition time and they were discussed in detail from the basic nucleation theories. The growth mechanism of ZnO nanorods on the SL is effectively investigated. The lateral growth was found in nanorods, due to lattice orientation effect. The hexagonal structural stabilization was also observed and discussed in detail. The Raman measurements confirm the wurtzite phase, high crystal quality and quantum confinement in ZnO nanorods.

## 1 Introduction

One dimensional (1D) semiconductor nanostructures have received more attention in recent days due to higher surface to volume ratio than 2D and 3D structures. The higher surface area enhances the reactivity and increases the absorption of photons, improved catalytic performance and sensitivity. 1D structure exhibits greater quantum confinement which improves the quantum transport in an allowed and unidirectional states and enhances the absorption and emission properties. ZnO is considered as a well-known material because of its multiple properties. It exhibits semiconducting, magnetic, piezoelectric, pyroelectric and lasing properties, among many others [1]. ZnO can be obtained in a wide variety of nanostructures such as nanoparticles, core-shell nanoparticles, tripods, tetrapods, hierarchical structures, nanoflower, nanosheets, vertically aligned nanosheets, nanowires, nanorods, nanotips, nanotubes and complex branched nanostructures [2].

ZnO has an excitonic binding energy of 60 meV at room temperature and it has the Bohr diameter of the excitons, 3.6 nm [3]. Due to the formation of strong excitons near band edges in 1D structure, ZnO effectively emits UV laser by recombination of exciton at valence band [1]. Since the ZnO nanostructure crystallised with high quality, it improves the electron transport by reducing electron hopping steps and thereby enhancing the electron mobility [4]. Vertically aligned ZnO nanorods provide higher interfacial area between the donor and the acceptor material by working as electrode which efficiently provide pathways for electron transport. Moreover the control of 1D structures at nanosize level provide novel and enhanced electrical, mechanical, chemical and optical properties. These special properties of ZnO is utilized in the fabrication of optoelectronics, acoustics, sensors, biomedical,

---

✉ R. Devaraj  
rdevaraj\_cbe@yahoo.co.in

<sup>1</sup> PG and Research Department of Physics, Government Arts College (Autonomous), Coimbatore, Tamilnadu 641018, India

<sup>2</sup> Department of Physics, Kongunadu Arts and Science College (Autonomous), Coimbatore, Tamilnadu 641029, India

electrochemical, new generation solar cells and other application devices [5–10]. In order to prepare 1D nanostructure for device fabrication, repeatability of the structure, surface to volume ratio, size, orientation, alignment, density and crystalline quality are to be optimised. The effective technique is already in practice to grow 1D nanostructure by using SL [11, 12]. SL especially in ZnO promotes anisotropic growth due to the reasons of polar nature and lattice matching with the surface of SL. Due to small wetting angle in heterogeneous growth on SL, more nucleation centres are created which reduces the formation of continuous film. The size of 1D structure depends on the interfacial energy between solute and crystal of SL which creates critical nucleus necessary for further growth. The SL may be a monoatomic layer [13] or thin film [12]. Several people have studied the effect of SL in the growth of 1D ZnO nanostructure [11–20]. Some reports conclude that SL supports the 1D nanostructure growth [13, 21] and vertical alignment of rods [17] but some of the reports failed to obtain the vertical alignment of rods on the SL [22]. In order to synthesis custom nanostructure one needs to understand the fundamental growth mechanism of nanostructure on seeded substrate. Moreover the resultant nanostructure depends on SL preparation conditions such as concentration, temperature, thickness and complex agent. Therefore this work has been formulated to study the importance of SL from the fundamental growth of nanostructure by varying concentration and deposition time.

## 2 Experimental details

The deposition of ZnO nanorods in the present work is carried in two steps. First, ZnO SL was prepared on pre-cleaned quartz substrate by jet nebulizer spray pyrolysis deposition technique [23] and then ZnO nanorods grown on seeded substrate by hydrothermal deposition technique.

### 2.1 Preparation of SL

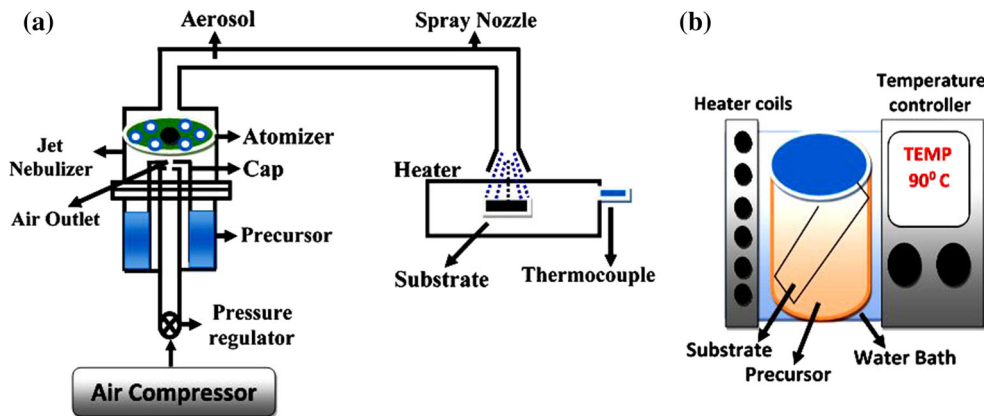
The experimental setup used for the preparation of SL is shown in the Fig. 1a. The precursor solution was prepared by dissolving zinc acetate compound [ $\text{Zn}(\text{CH}_3\text{COO})_2 \cdot 2\text{H}_2\text{O}$ ] in 10 ml of de-ionized water. The diameter of the spray nozzle is 1.5 cm and distance between substrate and spray nozzle was fixed at 3 cm. The solution spray rate was maintained at 0.5 ml per minute throughout the spray process. The pressure of carrier air gas was kept constant at 1 bar. The pre-cleaned quartz substrate was kept on the hot plate of spray setup and the temperature was set at 350 °C. After attaining desired temperature the prepared precursor solution was transferred into the jet nebulizer. The jet

nebulizer converts the liquid drop of precursor solution into aerosol via two ports. One port is designed for air flow and another port is used for the aerosol transport. The port at the centre is used for the transportation of air. The port diameter is decreased from 5 to 1 mm at the entrance where air is released. This set up of decreased diameter of the air hole is used to have venture effect of concentrating and increasing the pressure of air at the outlet. A small cap with a small hole at the centre is placed over the dimensions of air processing tube to suck the precursor solution and concentrating at the entrance of air outlet for spray. The regulated air with desired pressure crosses the venture tube, strikes the precursor solution projects the solution with high velocity. The high velocity solution is stopped by a semi-circular small solid projection at the centre. When it is stopped, the kinetic energy of the droplet is decreased and each droplet is divided into very fine droplets with a diameter of micrometer range. These micron diameter sized droplets cross the circular disc via the holes adjacent to the solid projection and transport to the nozzle tube. The mist like collection of these micron sized droplets are known as aerosol which is sprayed on the preheated quartz substrate at the end of nozzle tube. The advantage of using nebulizer spray pyrolysis method is that the droplets would be evaporated before reaching the substrate and only salt or precipitate reaches, spreads and condenses over the substrate. Therefore higher crystalline ordered SL is deposited on the substrate due to the thermal mobility of atoms. The SLs are prepared with 0.05 and 0.1 M concentrations of zinc acetate at a deposition time of 5, 10, 15 and 20 min.

### 2.2 Growth of ZnO nanorods

ZnO rods are grown on the SL by hydrothermal technique. The experimental setup is shown in the Fig. 1b. The precursor solution contains the equimolar  $\text{Zn}(\text{NO}_3)_2 \cdot 6\text{H}_2\text{O}$  and hexamethylenetetramine (HMTA) with 0.1 M are dissolved in de-ionized water. On constant stirring at room temperature for 30 min milky white coloured precursor is obtained. Then prepared SL is immersed into the solution by placing SL facing against wall of the beaker at 45° angle. The temperature of the bath was set at 90 °C and once the temperature is reached the precursor contained beaker is placed inside the bath and the deposition was carried out for 2 h. Due to the available thermal energy, the chemical bonding of the precursor solution will dissociate and releases  $\text{Zn}^{2+}$  and  $\text{O}^{2-}$  ions which migrate and attached to the seeded layer surface and finally form rod like morphology. The resulting films show light white colour with good adherence to the substrate. After deposition, the substrates are rinsed in de-ionized water and dried at room temperature overnight.

**Fig. 1** a Jet Nebulizer spray pyrolysis setup and b hydrothermal deposition setup



### 3 Results and discussion

#### 3.1 Structural studies

In order to study the role of SL on the growth of ZnO rod effectively, the SL is prepared with two conditions, (1) Different precursor concentrations of 0.05 and 0.1 M zinc acetate and (2) Different deposition time of 5, 10, 15 and 20 min with the respective concentration. The GIXRD patterns of ZnO rods grown on SL with 0.05 and 0.1 M at different deposition time are shown in Figs. 2 and 3. The diffraction peaks of the nanostructured films reveal the ZnO nanorods are crystallised in hexagonal wurtzite structure. No impurity peaks were observed in the pattern. The different concentrations at different deposition times show different orientations of ZnO nanorods on the surface of SL. In 0.05 M concentration (Fig. 2), the diffraction

peak along (002) plane is enhanced with increasing SL deposition time and it becomes predominant at 20 min. But in the case of 0.1 M concentration of zinc acetate, with increasing deposition time, initially the predominant orientation of crystallites along (002) plane is modified into many plane orientations. The results confirm the orientations of rods were strongly affected with SL precursor concentration as well as deposition time.

#### 3.2 Surface morphology and growth mechanism

Homogeneous nucleation of solid phase in liquid does not occur easily even though the ions are in supersaturated state or above supersaturated state. This is because, the homogeneous nucleation requires higher activation energy barrier through rapid cooling [24] and formation of solid

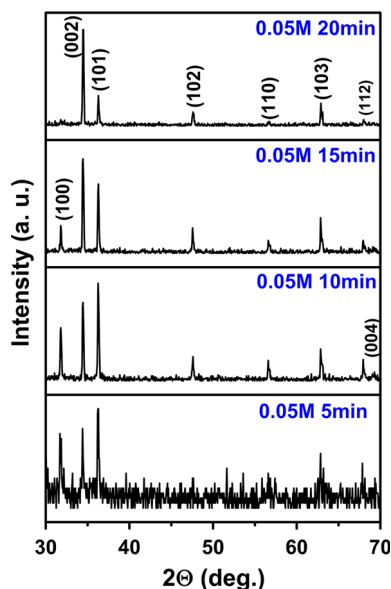


**Fig. 2** XRD pattern of ZnO rods grown on SL at different deposition time with 0.05 M concentration of zinc acetate

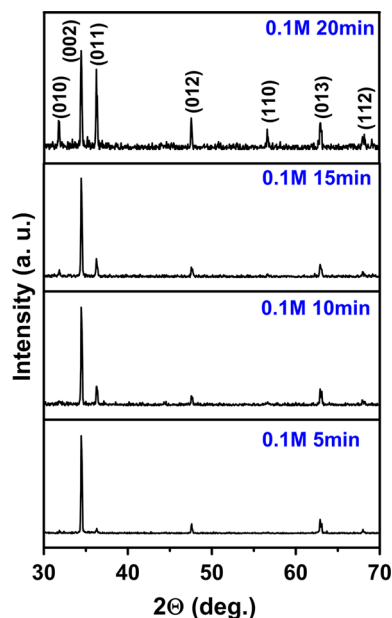


**Fig. 3** XRD pattern of ZnO rods grown on SL at different deposition time with 0.1 M concentration of zinc acetate

phase in liquid. Heterogeneous nucleation favours in the solution growth due to low contact angle between liquid–solid interface which reduces the activation energy barrier of growth on the substrate. Though heterogeneous nucleation on foreign surface is easier than the homogeneous nucleation, controlling random and complex nucleation on foreign surface is difficult due to lattice mismatch, strain at the interface of growing species and differential surface energy. Therefore in heterogeneous nucleation in the growth of nanostructure the SL will be deposited on the substrate with the same material as nanomaterial being grown on it. The advantage of same material as SL provides effective nucleation on favourable sites with minimal surface free energy which control morphology, texture and orientation of nanocrystals.

### 3.2.1 Effect of precursor concentration of SL

AFM images of ZnO nanorods grown on ZnO SL prepared at 0.05 and 0.1 M of zinc acetate at different deposition time are shown in Figs. 4 and 5. The mean square surface roughness of the films were calculated and the variation is given in Fig. 6. It is observed that nanorods grown on SL with the concentration of 0.05 M is having higher surface roughness value than it is grown on SL with the concentration 0.1 M. FESEM images of ZnO rods grown on ZnO SL prepared at 0.05 and 0.1 M of zinc acetate at various deposition time are shown in the Figs. 7 and 8. The ZnO rods grown on SL in the condition of 0.05 M in 5 min and 10 min deposition time (Fig. 7a, b) show nanorods grown unevenly on the SL whereas the ZnO rods grown in the condition of 0.1 M in 5 and 10 min deposition time (Fig. 8a, b) show ZnO nanorods grown uniformly throughout the surface. According to nucleation theories, the initial nucleus generally formed on foreign substrate by heterogeneous nucleation on energetically favourable sites. The nucleus will survive on surface after reaching the critical size with less surface free energy and below which it dissolves [25]. Energetically, formation of nucleation sites in the condition of 0.05 M concentration at 5 and 10 min deposition on the quartz substrate are inadequate throughout the substrate. The less number of available atomic species in the low concentration solution and less time period of deposition not forming nucleation on the entire surface of the substrate is due to higher activation energy barrier and lattice mismatch. Therefore the density of the rod on the surface is less due to the less number of nucleation sites on the SL. When the concentration is increased to 0.1 M, the available atomic species in the growth and time interval of 5 and 10 min is increased and hence the formation of nucleation on the surface of quartz substrate is increased. Further in the time period, lateral growth of Frank-van der Merwe takes place predominantly

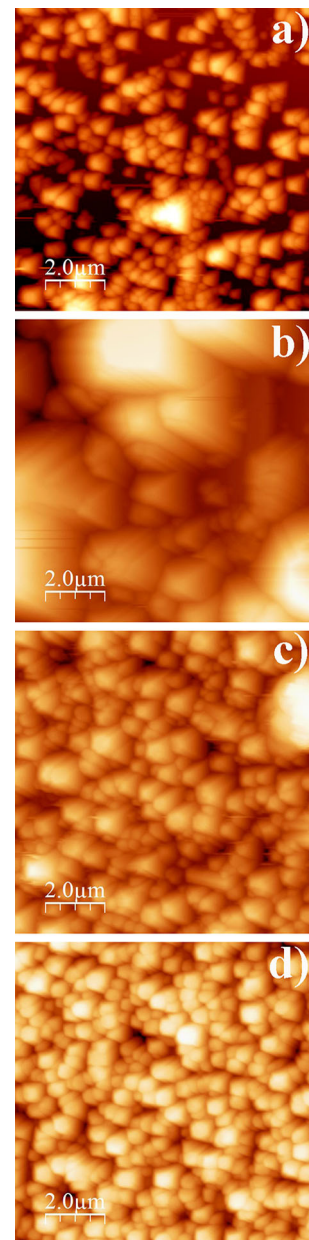


**Fig. 4** Two dimensional AFM images of ZnO rods grown on SL at different deposition time as **a** 5 min, **b** 10 min, **c** 15 min and **d** 20 min with 0.05 M concentration of zinc acetate

in spray pyrolysis technique than oriented growth adjacent to nucleus on the surface which forms continuous film with more energetically favourable nucleation sites on the surface for further growth. Hence the growth at the concentration of 0.1 M in SL shows nanorods uniformly grown on the surface of SL (Fig. 8a, b).

### 3.2.2 Effect of SL deposition time

Figures 7 and 8 depict the surface morphology of ZnO nanorods grown on ZnO SL at various deposition times.



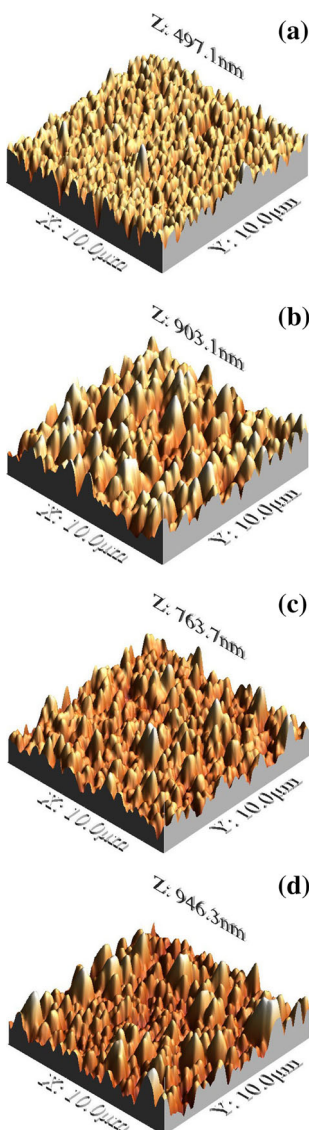


**Fig. 5** Three dimensional AFM images of ZnO rods grown on SL at different deposition time as **a** 5 min, **b** 10 min, **c** 15 min and **d** 20 min with 0.1 M concentration of zinc acetate

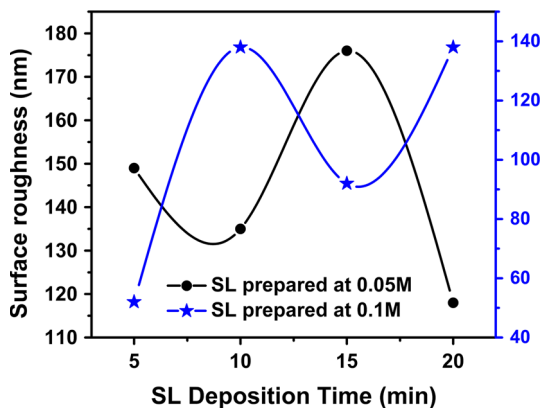


**Fig. 6** Surface roughness calculated from AFM

The mechanism of ZnO nanorod grown on ZnO SL by hydrothermal method was reported elsewhere [26, 27]. It was observed from the XRD patterns that ZnO nanorods were crystallised in wurtzite phase. In the wurtzite structure of ZnO, the top and bottom surfaces are normally terminated with negative charge by  $O^{2-}$  ions and positive charge by  $Zn^{2+}$  ions. Hence the SL surface is filled with energetically favourable nucleation sites due to the lattice matching and the polar nature of ZnO. The nucleus formation on the SL surface is based on the active surface area that is surface free energy of molecules.

At 0.05 M concentration and 5 min deposition time, the density of ZnO nanorods on the surface of SL is low (Fig. 7a), and by increasing deposition time to 10 min, the density of the rod was increased with the increasing of size and diameter (Fig. 7b). The increase in density is due to the increase in the nucleation sites on the surface of SL and increase in the size of rod is due to the increase of secondary nucleation along the direction of rod. Further increase in deposition time of SL results the growth of nanorods uniformly throughout the surface of SL with improper alignment (Fig. 7c). The alignment and orientation of nanorods are improved when grown on SL at a deposition time of 20 min (Fig. 7d) and it is observed that almost all ZnO hexagonal rods are vertically aligned in (002) plane in c-axis. This vertical growth of ZnO can be understood by growth mechanism. In ZnO, polar surfaces of (0001) plane terminated with  $Zn^{2+}$  and (000 $\bar{1}$ ) plane terminated with  $O^{2-}$  having higher surface energy of  $4.00 J/m^2$  which is greater than the surface energy of  $2.32 J/m^2$  of non-polar facets (0 $\bar{1}00$ ) and (2 $\bar{1}\bar{1}0$ ) [28]. Hence higher surface energy facets (0001) and (000 $\bar{1}$ ) are more reactive which attracts the opposite ions in the solution and the growth takes by forming critical nucleus by secondary nucleation on the surface of polar facets. Hence the surface energy of the polar facets are minimized further and further by coordinating with opposite ions and the nanorod growth takes place along c-axis by alternatively stacking the layers of zinc and oxygen ions. Since the surface energy of the non-polar side facets {01 $\bar{1}0$ } are comparatively less than the polar facets, growth normally not taking place on the lateral sides.

In the case of growth of nanorods on ZnO SL in 0.1 M concentration from 5 to 20 min show converse effect to the surface morphology of 0.05 M concentration. The nanorods grown on SL at 5 min deposition time show more alignment in the vertical direction (Fig. 8a). On increasing SL deposition time, the vertical alignment of nanorods are deteriorated and the rods start to coalesce together (Fig. 8b, c). This might be due to the crystal defects of dislocation of atoms at the interface of rods.

The growth on SL at 20 min deposition time, the bigger rods appeared between the dense of smaller rods (Fig. 8d). It was observed that bigger rods have grown by

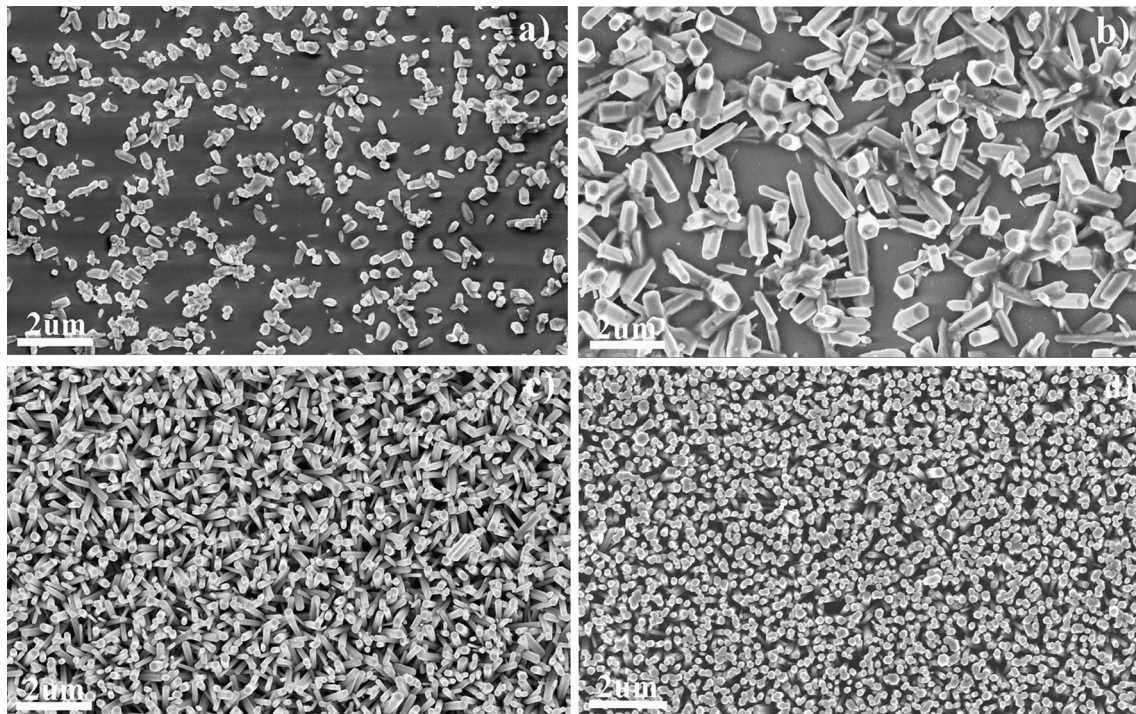


**Fig. 7** FESEM images of ZnO rods grown on SL at different deposition time as **a** 5 min, **b** 10 min, **c** 15 min and **d** 20 min with 0.05 M concentration of zinc acetate

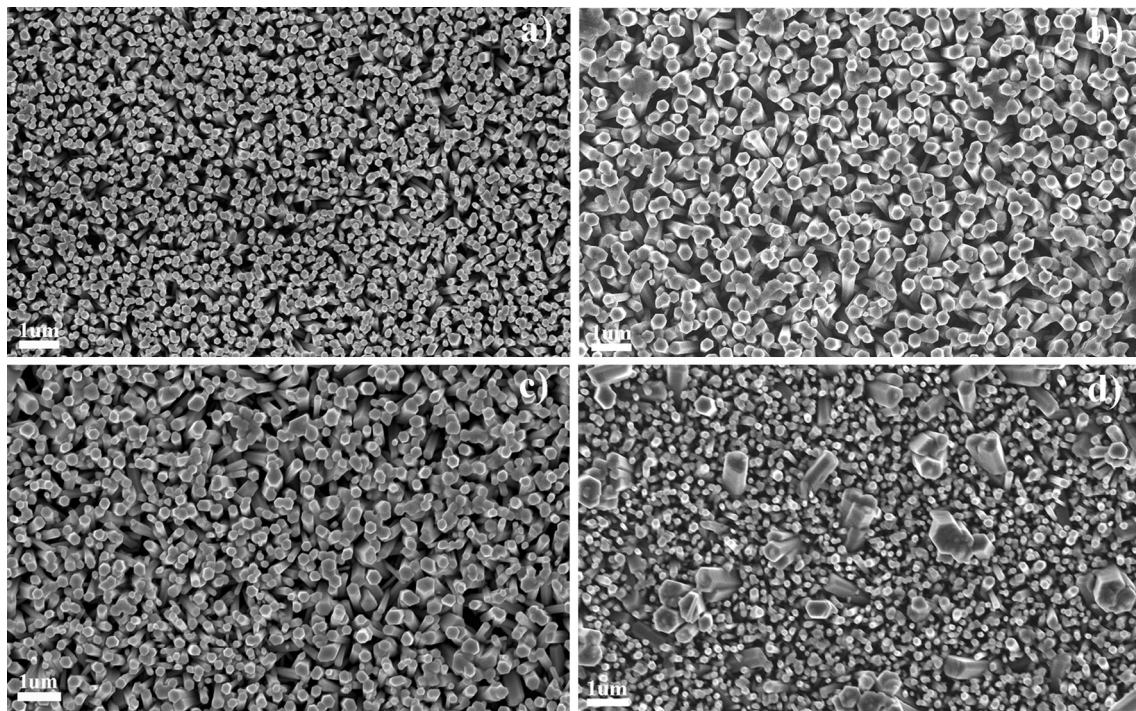


**Fig. 8** FESEM images of ZnO rods grown on SL at different deposition time as **a** 5 min, **b** 10 min, **c** 15 min and **d** 20 min with 0.1 M concentration of zinc acetate

coalescence of one or more nearby rods due to lattice orientation effect. In most cases, the orientation effect was found along c-axis and only in some cases it was found in

lateral sides [29]. In the growth of nanorods, the nucleus are formed at the nucleation centres and started to grow normally along the c-axis. The lattice orientation and



alignment of rods are dependent on the contact angle of nucleus on the surface of SL. Wherever the growth takes place by secondary nucleation in a manner that the rods having the lattice planes grown parallel to the same planes of nearby rod, due to the lattice orientation attachment, the particles at the interface is dislocated and coalesce evenly along the growth direction throughout the interface. The hexagonal structure stabilization takes place further between coalesced rods by dislocation of atoms and forms bigger rods with the stabilized hexagonal structure. Finally the ordered hexagonal crystal shape is obtained from the defects of disorder. In general lateral growth is not taking place due to the less surface free energy of non-polar facets, but lattice orientation attachment causes the lateral growth by coalescence of oriented rods. It can be observed from Fig. 8d that the average diameter of small rods were found to be 197 nm and big rods were found to be 602 nm. Hence it is understood that almost 400 nm is increased in the lateral side by lattice orientation attachment.

The variation of rod diameter deposited on different SL concentration and deposition time is shown in Fig. 9. With increasing SL deposition time, rod diameter varying from 175 to 426 nm for a concentration of 0.05 M and varying from 157 to 602 nm for a concentration of 0.1 M. The variations of diameter of rods depend on critical nucleus on the SL surface. The size of the critical nucleus depends on the interfacial energy between solute and crystal. When the interfacial energy is less, the critical nucleus size is less and vice versa. It is observed that the SL prepared in both the concentrations at 5 min deposition time show nanorods of less diameter.

### 3.3 Raman studies

Wurtzite hexagonal-shaped ZnO belongs to the  $C_{6v}^4$  ( $P6_3mc$ ) symmetry group, with two formula units per primitive cell, where all of the atoms are occupying the

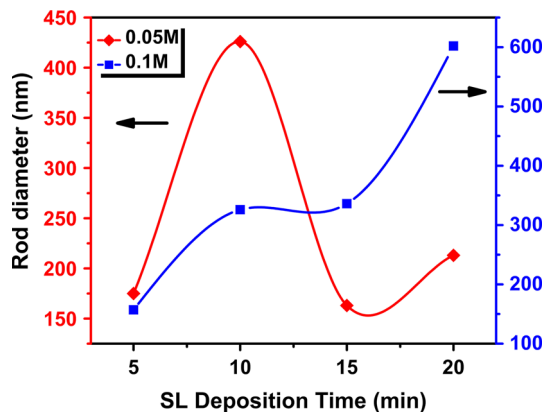


Fig. 9 Rod diameter calculated from FESEM images

$C_{3v}$  sites [30]. Group theory predicts that the single crystalline ZnO has eight sets of optical phonons near the centre of the Brillouin zone, and hence it is classified as  $\Gamma = A_1 (TO,LO) + 2B_1 + E_1 (TO,LO) + 2E_2$  [31]. Among these, the  $A_1$  and  $E_1$  modes are both Raman and infra-red active. Moreover, these  $A_1$  and  $E_1$  are polar and split into two transverse optical (TO) and longitudinal optical (LO) phonons.  $E_2$  modes are Raman active only while the  $B_1$  modes are silent. Figures 10 and 11 show the Raman spectra of ZnO nanorods grown on SL with concentration of 0.05 and 0.1 M of zinc acetate. Totally five optical phonon modes were observed in both concentrations around 333, 381, 439, 489 and 582  $cm^{-1}$ . By comparing the peaks with bulk ZnO, the peaks at 333, 381, 439, 489 and 582  $cm^{-1}$  are assigned as  $E_2(\text{high})-E_2(\text{low})$ ,  $A_1(\text{TO})$ ,  $E_2(\text{High})$ , LA and  $E_1(\text{LO})$ . Among the five peaks,  $E_2(\text{High})$  peak was predominant and other peaks were weak. The appearance of multiphonon scattering confirms the quantum confinement in the ZnO nanorods [32].  $A_1(\text{TO})$  and  $E_2(\text{High})$  modes are fundamental Raman active modes.  $A_1(\text{TO})$  is polar Raman active mode.  $E_2(\text{High})$  optical phonon mode of ZnO, relates the characteristic wurtzite phase of ZnO and also crystalline property. Here in both concentrations, the peak intensity of  $E_2(\text{high})$  was predominant over the other peaks which indicates that the obtained ZnO nanorods were in hexagonal wurtzite phase with high crystalline quality. The peak intensity of  $E_2(\text{high})$  increases in a condition of SL deposited at 15 and 20 min. Figures 10 and 11 show the improved crystal quality of the rods. Compared to  $E_2(\text{high})$  peak position of bulk (444  $cm^{-1}$ ), the obtained nanorods are red shifted with 5  $cm^{-1}$ . The appearance of  $E_1(\text{LO})$  optical phonon mode reveals c-axis ZnO nanorods of wurtzite phase was perpendicular to the substrate. LA mode around 489  $cm^{-1}$  is a silent mode in ZnO.

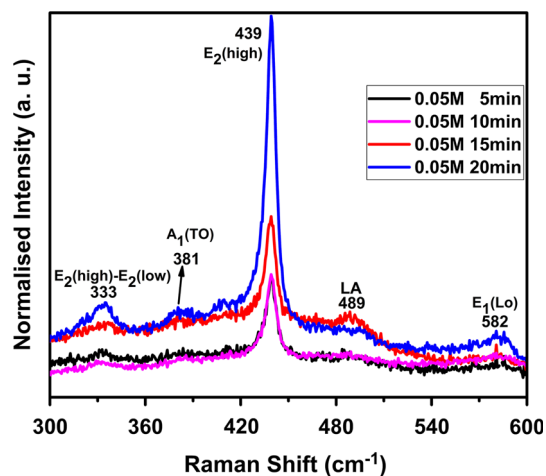
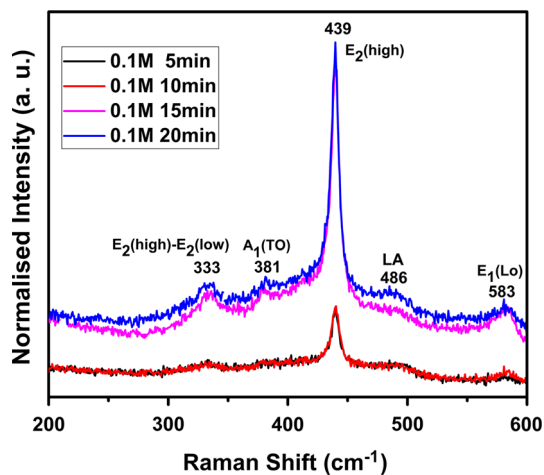


Fig. 10 Raman spectrum of ZnO rods grown on SL at 0.05 M



**Fig. 11** Raman spectrum of ZnO rods grown on SL at 0.1 M

#### 4 Conclusion

The role of SL on the growth of ZnO nanorods was investigated by preparing SL with two concentrations of 0.05 and 0.1 M of zinc acetate by jet nebulizer spray pyrolysis technique at different deposition time of 5, 10, 15 and 20 min. The ZnO nanorods are grown on the ZnO seeded substrate by hydrothermal method. The influence of SL in the growth of ZnO nanorods with respect to SL concentration and deposition time were studied with various characterization tools.

The findings show that the orientation of crystallites along (002) direction was increased with the increasing of SL deposition time from 5 to 20 min for 0.05 M concentration of zinc acetate. The converse effect was found in nanorods grown with 0.1 M concentration of zinc acetate with 0.05 M zinc acetate on increase of deposition time. The various morphologies were obtained on the surface of SL with different concentrations and deposition time and were discussed in detail from the basic nucleation theories. The growth mechanism of ZnO nanorods on the SL was effectively investigated. Orientation effect was found in ZnO rods on SL deposited at 20 min in 0.1 M concentration. The orientation effect leads to lateral growth by coalescence of two or more rods. Hexagonal structure stabilization is also observed with dislocation of atoms between the rods and in an average 400 nm is increased in lateral side by lattice orientation attachment. Overall it was found that SL is modifying the surface morphology, alignment of rods, size of rods and lateral growth.

**Acknowledgments** The authors would like to acknowledge Dr.P. Elango, Associate Professor, Department of Physics, Government Arts College, Coimbatore and Dr.K.Saravanakumar, Assistant Professor, Department of Physics, Kongunadu Arts and Science College, Coimbatore for the support extended in this research.

#### References

1. D. Hofstetter, R. Theron, A.-H. El-Shaer, A. Bakin, A. Waag, *Appl. Phys. Lett.* **93**, 101109 (2008)
2. X. Wang, J. Song, Z.L. Wang, *J. Mater. Chem.* **17**, 711 (2007)
3. D.P. Norton, Y.W. Heo, M.P. Ivill, K. Ip, S.J. Pearton, M.F. Chisholm, T. Steiner, *Mater. Today* **7**, 34 (2004)
4. D.J. Milliron, S.M. Hughes, Y. Cui, L. Manna, J.B. Li, L.W. Wang, A.P. Alivisatos, *Nature* **430**, 190 (2004)
5. A. Tsukazaki, A. Ohtomo, T. Onuma, M. Ohtani, T. Makino, M. Sumiya, K. Ohtani, S.F. Chichibu, S. Fuke, Y. Segawa, H. Ohno, H. Koinuma, M. Kawasaki, *Nat. Mater.* **4**, 42 (2005)
6. Y.R. Ryu, J.A. Lubguban, T.S. Lee, H.W. White, T.S. Jeong, C.J. Youn, B.J. Kim, *Appl. Phys. Lett.* **90**, 131115 (2007)
7. J.-I. Song, J.-S. Park, H. Kim, Y.-W. Heo, J.-H. Lee, J.-J. Kim, G. M. Kim, B. D. Choi, *Appl. Phys. Lett.* **90**, 022106 (2007)
8. Z. Zhang, N.W. Emanetoglu, G. Saraf, Y. Chen, P. Wu, J. Zhong, Y. Lu, J. Chen, O. Mirochnitchenko, M. Inouye, *IEEE Trans. Ultrason. Ferroelectr. Freq. Control* **53**, 786 (2006)
9. H.T. Wang, B.S. Kang, F. Ren, L.C. Tien, P.W. Sadik, D.P. Norton, S.J. Pearton, J. Lin, *Appl. Phys. Lett.* **86**, 243503 (2005)
10. Z.L. Wang, *J. Phys. Condens. Matter* **16**, R829 (2004)
11. J. Song, S. Lim, *J. Phys. Chem.* **111**, 596 (2007)
12. S.-F. Wang, T.-Y. Tseng, Y.-R. Wang, C.-Y. Wang, L. His-Chan, *Ceram. Int.* **35**, 1255 (2009)
13. Q. Li, V. Kumar, Y. Li, H. Zhang, T.J. Marks, R.P.H. Chang, Fabrication of ZnO nanorods and nanotubes in aqueous solutions. *Chem. Mater.* **17**, 1001 (2005)
14. P.K. Giri, S. Dhara, R. Chakraborty, *Mater. Chem. Phys.* **122**, 18 (2010)
15. H. Lee, J.H. Shin, J. Chae, J.B. Kim, T.H. Kim, K.B. Park, *Electron. Mater. Lett.* **9**, 357 (2013)
16. Z. Liu, J. Ya, E. Lei, *J. Solid State Electrochem.* **14**, 957 (2010)
17. M. Guo, P. Diao, S. Cai, *J. Solid State Chem.* **178**, 1864 (2005)
18. Y. Tao, F. Ming, A. Zhao, D. He, Y. Wang, *J. Alloys Compd.* **489**, 99 (2010)
19. H. Ghayour, H.R. Rezaie, S.H. Mirdamadi, A.A. Nourbakhsh, *Vacuum* **86**, 101 (2011)
20. Y.-J. Lee, T.L. Sounart, J. Liu, E.D. Spörcke, B.B. McKenzie, J. W.P. Hsu, J.A. Voigt, *Cryst. Growth Des.* **8**, 2036 (2008)
21. N.S. Ridhuan, K.A. Razak, Z. Lockman, A.A. Aziz, *PLoS One* **7**, 11 (2012)
22. A. Sugunan, H.C. Warad, M. Boman, J. Dutta, *J. Sol-Gel. Sci. Technol.* **39**, 49 (2006)
23. C. Ravidhas, B. Anitha, A. Moses Ezhil Raj, K. Ravichandran, T. C. Sabari Girisun, K. Mahalakshmi, K. Saravanakumar, C. Sanjeeviraja, *J. Mater. Sci. Mater. Electron.* **26**, 3573 (2015)
24. L. Vayssieres, *Int. J. Nanotechnol.* **1**, 1 (2004)
25. N.T. Thanh, N. Maclean, S. Mahiddine, *Chem. Rev.* **114**, 7610 (2014)
26. S. Xu, Z.L. Wang, *Nano Res.* **4**, 1013 (2011)
27. D. Polsongkram, P. Chamnink, S. Pukird, L. Chow, O. Lupan, G. Chai, H. Khallaf, S. Park, A. Schulte, *Phys. B* **403**, 3713 (2008)
28. A. Wander, F. Schedin, P. Steadman, A. Norris, R. McGrath, T.S. Tumer, G. Thornton, N.M. Harrison, *Phys. Rev. Lett.* **86**, 3811 (2001)
29. C. Pacholski, A. Kornowski, H. Weller, *Angew. Chem. Int. Ed.* **41**, 1188 (2002)
30. C. Klingshirn, J. Fallert, H. Zhou, J. Sartor, C. Thiele, F. Maier-Flaig, D. Schneider, H. Kalt, *Phys. Stat. Solidi B* **247**, 1424 (2010)
31. Q. Li, J. Bian, J. Sun, J. Wang, Y. Luo, K. Sun, Y. Dongqi, *Appl. Surf. Sci.* **256**, 1698 (2010)
32. M. Soosen Samuel, J. Koshy, A. Chandran, K.C. George, *Ind. J. Pure Appl. Phys.* **48**, 703 (2010)